Received: 17 October 2021 | Revised: 2 April 2022 | Accepted: 20 April 2022

DOI: 10.1002/ldr.4309

RESEARCH ARTICLE

WILEY

Determination of the threshold velocity of soil wind erosion using a wind tunnel and its prediction for calcareous soils of Iran

Mahrooz Rezaei[1] | Monireh Mina[2] | Yaser Ostovari[3] | Michel J. P. M. Riksen[4]

[1]Meteorology and Air Quality Group, Wageningen University & Research, Wageningen, The Netherlands

[2]Department of Soil Science, School of Agriculture, Shiraz, Iran

[3]Chair of Soil Science, Research Department of Ecology and Ecosystem Management, TUM School of Life Sciences – Weihenstephan, Technical University of Munich, Freising, Germany

[4]Soil Physics and Land Management Group, Wageningen University & Research, Wageningen, The Netherlands

Correspondence
Mahrooz Rezaei, Meteorology and Air Quality Group, Wageningen University & Research, PO Box 47, 6700 AA Wageningen, The Netherlands.
Email: mahrooz.rezaei@wur.nl

Abstract

Determination of the threshold velocity (TV) is a crucial step for wind erosion evaluation. Due to the difficulties of direct field measurements, pedotransfer functions (PTFs) and easily measurable soil properties could be used to save time and cost in predicting TV. Therefore, the present study was conducted to predict the TV using PTFs and to assess its influential parameters for calcareous soils of Fars Province, southern Iran. To this end, the TV was measured by a portable wind tunnel at 72 locations in different land uses and soil types across the study site. Various physicochemical and mechanical soil properties were used to develop six PTFs using multiple linear regression. Results showed that the TV varied from 3.0 m s^{-1} in poor rangelands to 12.83 m s^{-1} in saline lands. Soil surface shear strength (SS) with a correlation coefficient of 0.85 was the most influential parameter affecting the TV, followed by aggregate mean weight diameter (MWD). Results of the predictive models revealed that PTF 5, which was developed using SS and penetration resistance (PR;$R^2 = 0.86$, RMSE = 0.85 m s^{-1}), and PTF 6, which was developed using MWD and PR ($R^2 = 0.81$, RMSE = 1.07 m s^{-1}), had the highest performance for predicting the TV. PTF 5 was selected as the final model for predicting the TV since it only needed easily measurable soil properties without soil sample collection. We concluded that the use of PTFs could be an applicable alternative way to predict the TV, particularly at large scales.

KEYWORDS

dust, pedotransfer function, regression, shear strength, soil erosion

1 | INTRODUCTION

Wind erosion and dust production are major challenges related to climate change in the World and especially in the Middle East. Iran is located in the arid and semiarid belt (Chappell et al., 2018; Moradi et al., 2011) and is considered as an important source of dust in this region (Shao, 2008). Wind erosion is a nonlinear process affected by many factors such as soil properties, surface roughness (SR), soil moisture, climate, and topography (Li et al., 2015). It is directly related to human health due to the entry of fine particles through the respiratory system (Bento et al., 2017). In addition, it erodes fertile soils, resulting in a decrease in food production (Sharratt & Vaddella,

2014). In arid and semiarid areas, the assessment of the threshold velocity (TV) of wind where soil particles start to move is used as a key indicator for the wind erosion risk (Li et al., 2010). The TV is significantly linked to soil properties (Morshedi Nodej & Rezazadeh, 2018). Chepil (1950) related wind erodibility of soils to dry aggregate structure indices. In literature, other factors have been well-introduced as the most influential soil properties affecting the TV: soil particle size distribution (Munkhtsetseg et al., 2016; Sweeney et al., 2016; Van Pelt et al., 2017; Von Holdt et al., 2019); aggregate stability (Zamani & Mahmoodabadi, 2013); soil organic matter (OM; Sirjani et al., 2019); and calcium carbonate equivalent (CCE; Kheirabadi et al., 2018; Kouchami-Sardoo et al., 2020). In addition to these soil characteristics, researchers also looked at penetration resistance (PR; Kouchami-Sardoo et al., 2020; Mina et al., 2020) and SR, a measure of the microrelief of the surface (Gillies et al., 2006; Moreno et al., 2010; Sankey et al., 2010; Vázquez et al., 2005; Yan et al., 2015) in relation to the TV. Soil crusts increasing the resistance of the soil surface to shear stress is another vital factor in controlling wind erosion (Mina et al., 2020; Zhang et al., 2006).

In past decades, portable wind tunnels have been frequently used to measure wind erosion in natural conditions for various purposes (Van Pelt & Zobeck, 2013). Li et al. (2010) determined the TV using different methods including wind tunnel, airgun, compressive strength, and soil roughness (SR) in California, USA. They concluded that the wind tunnel and compressive strength methods satisfactorily estimate the TV. As measuring the TV in the field is labour-intensive, time-consuming, and costly, it would be advantageous if the TV could be estimated indirectly. This is especially important when large areas are susceptible to wind erosion. Moreover, investigation of the spatial heterogeneity of the TV is difficult when using wind tunnels (Li et al., 2015).

Considering these field restrictions, there is a growing interest in estimating the TV using easily measurable soil properties, the so-called pedotransfer function (PTF). The use of PTFs for the accurate estimation of the TV could be a useful tool in defining soil conservation strategies against wind erosion. It is particularly useful for large areas in respect of saving time, energy, and money (Kouchami-Sardoo et al., 2019; Kumar et al., 2008).

One of the most common methods that has been proven to be a promising technique for developing PTFs is multiple linear regression (MLR; Liao et al., 2011). The MLR model describes how a single response variable depends linearly on a number of predictor variables. The MLR has been used for predicting various soil properties such as soil water retention curve and saturated soil hydraulic conductivity (Moazenzadeh & Ghahraman, 2016; Wagner et al., 2001), bulk density (Brahim et al., 2012), soil aggregate stability (Shi et al., 2020), soil infiltration and cation exchange capacity (Kashi et al., 2014), soil erodibility (Ostovari et al., 2016), and soil loss tolerance (Ostovari et al., 2020). However, there has been no study on predicting the TV using PTFs models.

Iran is located in the semiarid and arid belts, and two-thirds of Iran have desert conditions (Kouchami-Sardoo et al., 2019). Fars Province, which is located in southern Iran, is an important agricultural province for producing strategic crops including wheat and rice. According to the Natural Resources Organization of Fars Province (Sirjani et al., 2019), due to the climate conditions, wind erosion occurs in most parts of Fars and desertification has increased over the recent decades. Thirty critical centres of wind erosion have been identified in the Fars. Many lakes in Fars Province have dried-up and become a potential source of fine sediment particles containing salt and other pollutants and wind can turn these areas into dust centres. Therefore, the study of wind erosion and its related processes has received growing attention in this region. Hence, such studies are needed to guide the decision-makers to implement support actions to conserve soil against wind erosion in these areas. Therefore, the present work attempted to: (1) determine the TV by a portable wind tunnel in different land uses and soil types; and (2) develop some PTFs using easily measurable soil properties including field-based and laboratory-based soil properties using the MLR method with the emphasis on the concept of PTFs.

2 | MATERIALS AND METHODS

2.1 | Study area

Fars Province is located in the south-central region of Iran (Figure 1), between 27°2′ and 31°42′ latitude and 50°42′ and 55°36′ longitude, covering an area of 133,299 km^2. The mean annual precipitation varies from 100 mm in the southern part to 400 mm in the northern part of the study site. Fars Province has an arid and semiarid climate according to the De Marten aridity index (Rezaei et al., 2016). There are three main meteorological stations (Figure 1) located at Abadeh (31°11′N and 52°40′E), Eghlid (30°54′N and 52°38′E), and Shiraz (29°32′N and 52°36′E). To illustrate the occurrence of high wind events in the province, the maximum recorded wind velocity (at 10 m height) at these meteorological stations is presented in Figure 2. The maximum wind velocity varied from 30 m s^{-1} in Abadeh and Shiraz to 45 m s^{-1} in Eghlid. In addition, several dust storm events have been reported in this province, such as on July 17, 1998, August 13, 2001, April 24, 2008, February 28, 2009, August 28, 2013, and May 13, 2018 (Abbasi et al., 2021; Mazidi et al., 2015).

In this study, 72 locations in different geographical landscapes across Fars Province were selected. According to the soil taxonomy classification, soil types of the study locations were mainly Aridisols (~24%), Entisols (~21%), and Inceptisols (~55%). Based on field and image monitoring, land uses in the study sites included irrigated agricultural land (~33%), poor rangeland (<5% vegetation cover; ~24%), moderate rangeland (5%–15% vegetation cover; ~34%), and saline land (~8%). The agricultural lands were mostly seasonal and abandoned lands. The slope of all the study areas was less than 1% (Natural Resources Organization of Fars, 2019).

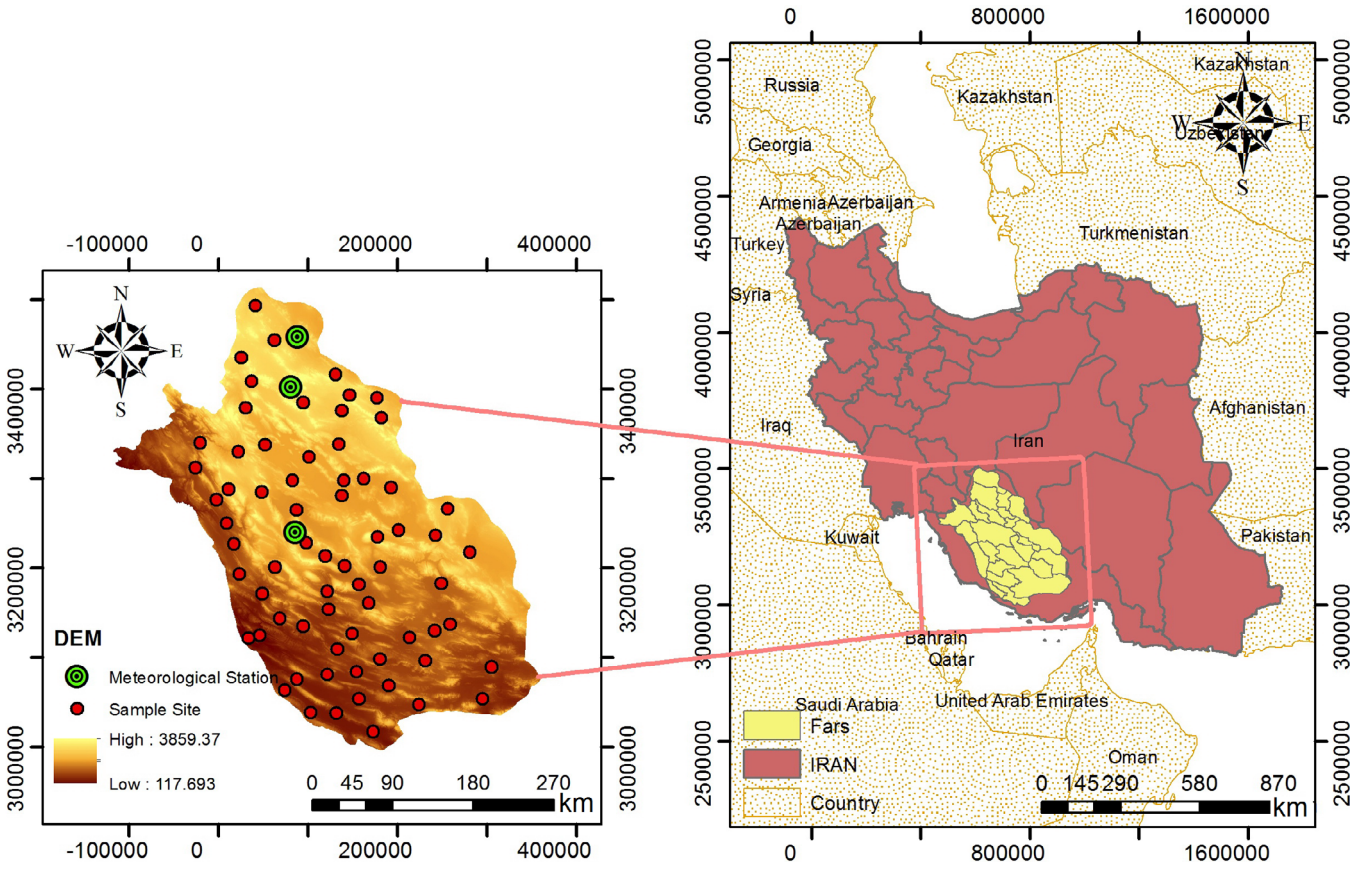

FIGURE 1 Map of Fars Province, Iran and locations of the sampling sites and meteorological stations (UTM, zone 39). DEM, digital elevation model

2.2 | Soil samples

Soil samples were collected from a thin topsoil layer (0–3 cm) at each experimental location in the summer of 2019. Soil samples were taken randomly in three replicates at the nearest place adjacent to the wind tunnel. The collected samples were transferred to the laboratory, air-dried, and then sieved <2 mm for the soil analysis.

2.3 | Soil analysis

At each sampling site (Figure 1), the PR, SR, and shear strength (SS) were measured. Ten replicate experiments in a radius of 1 m of the wind tunnel were considered (Figure 3a). Measurements were carried out in the same soil type and land use and in the places nearest to the wind tunnel but not overlapped with footprints of the wind tunnel tests, as the wind tunnel test would cause disturbance to the soil surface. A pocket penetrometer model ELE, 29-3729 was used to measure PR according to the methodology by Bradford (1986). The chain method (Saleh, 1993) was carried out for measuring the SR (Figure 3b). The SR was then calculated as follows:

$$R = \left(1 - \frac{L2}{L1}\right) * 100 \quad (1)$$

Where: $L1$ is the length of chain required to span roughness element (s) for a horizontal distance $L2$.

The SS of the surface *soil* is an important soil mechanical property to predict its resistance against the shear force created by the wind (Zhang et al., 2018). The SS of the soil surface was measured using a pocket Torvane shear apparatus model V015.HM-504A (Figure 3c).

Besides field measurements, soil texture was measured using the hydrometer method (Page et al., 1992). Aggregate mean weight diameter (MWD) was obtained using the dry-sieving method (Kemper & Rosenau, 1986). The CCE and soil OM were measured by the HCl back-titration (Nelson, 1982) and the LOI methods (Hoogsteen et al., 2015), respectively. Electrical conductivity (EC) of saturated extract was determined by the EC-meter.

2.4 | Wind tunnel experiments

Extensive wind tunnel experiments were carried out at 72 locations with three replicates providing a variety of soils with different potential for wind erosion. All three replications were done on the same surface type as close to each other as possible, but not overlapped with footprints of previous wind tunnel tests, as the wind tunnel test would

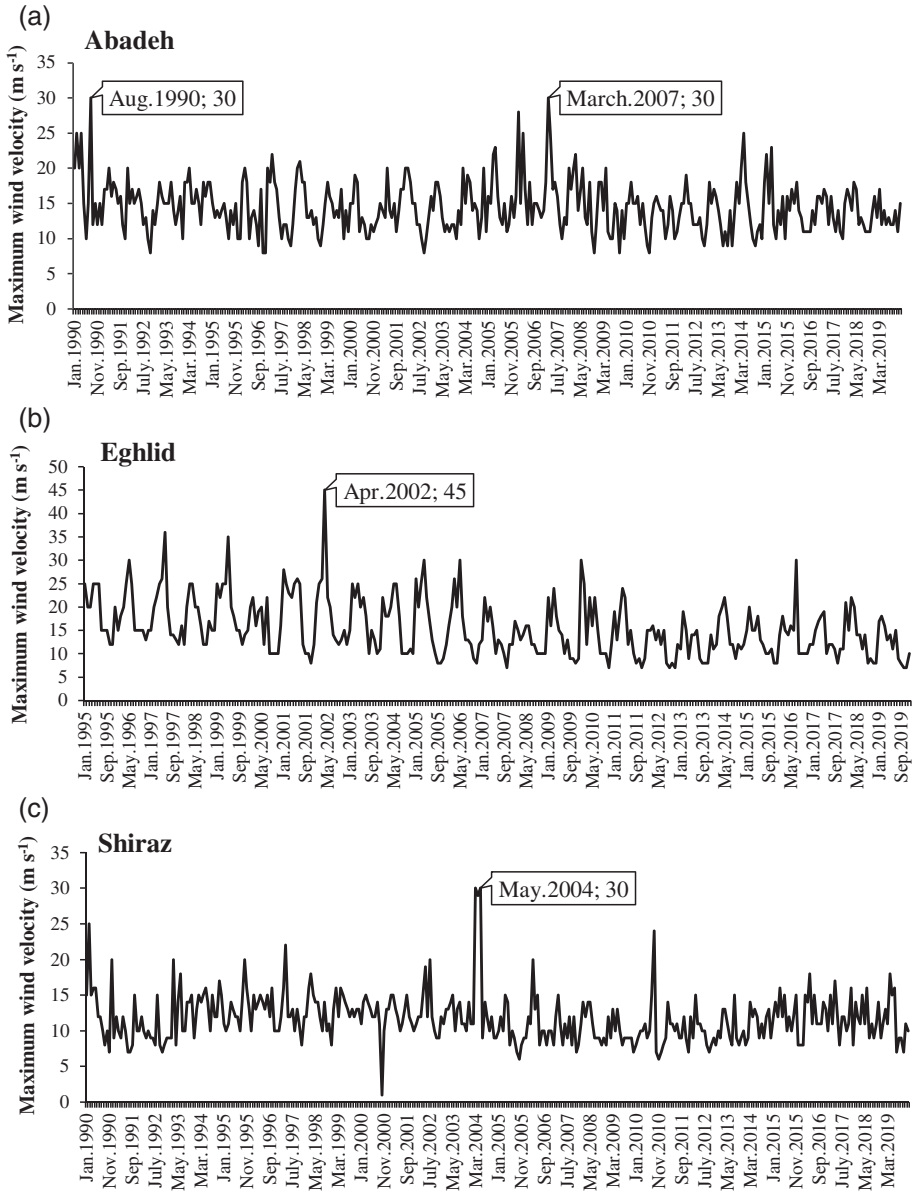

FIGURE 2 Maximum wind velocity (m s^{-1}) (at 10 m height), at (a) Abadeh, (b) Eghlid, and (c) Shiraz meteorological stations

cause disturbance to the soil surface. Measurements were carried out on flat areas of land with little to no vegetation without any surface disturbance in the summer of 2019 when the soil was dry. During the fieldwork, one extra soil sample was collected for the measurement of initial soil moisture content. Results proved that the soil moisture contents (mean = 0.98%) were below the highest soil moisture allowed to guarantee wind erosion (Bento et al., 2017). To determine TV for the selected sites, a portable wind tunnel was used. The wind tunnel was positioned on intact soil surface in the direction of the prevailing wind. The details of the wind tunnel can be found in Kouchami-Sardoo et al. (2020). This wind tunnel has a work section of 2.5 m long with a cross section of 0.3 * 0.3 m^2, a test area of 1 m in length and 0.3 m in width, and an 8-m sediment collector that has a two-layer cyclone made of plastic. This plastic catcher has no effect on the wind conditions due to the holes with 0.1 m diameter that have been created on the top part of the outer plastic tube to egress the wind flow. After deposition of the wind-eroded particles at the sediment catcher, the clean wind passes through the holes. According to the wind velocity calibration for the wind tunnel, the wind velocity profile obeying the Law of the wall is well established at a distance of about 1.5 m downwind of the wind flow conditioning section, where the measurement area is placed. Besides, a handy digital wind meter was used to check the wind velocity generated by the wind tunnel before each wind tunnel experiment. The same device has been employed successfully in other wind erosion studies (Azimzadeh et al., 2008; Kouchami-Sardoo et al., 2020; Mina et al., 2021; Naghizade Asl et al., 2019; Rezaei et al., 2019; Sirjani et al., 2019). TV was determined based on the observational method by gradually increasing the wind velocity in the wind tunnel to reach the TV until the forward movement of the soil particles was observed. (Belnap et al., 2007; Rezaei et al., 2019; Figure 3d). This forward movement was observed through the glass window of the test section of the wind tunnel. This procedure was again repeated three times to gain the representative and accurate TV. Worth to mention that minimum, mean, and maximum of standard deviation (SD) for TV were 0.00, 0.26, and 0.58, respectively.

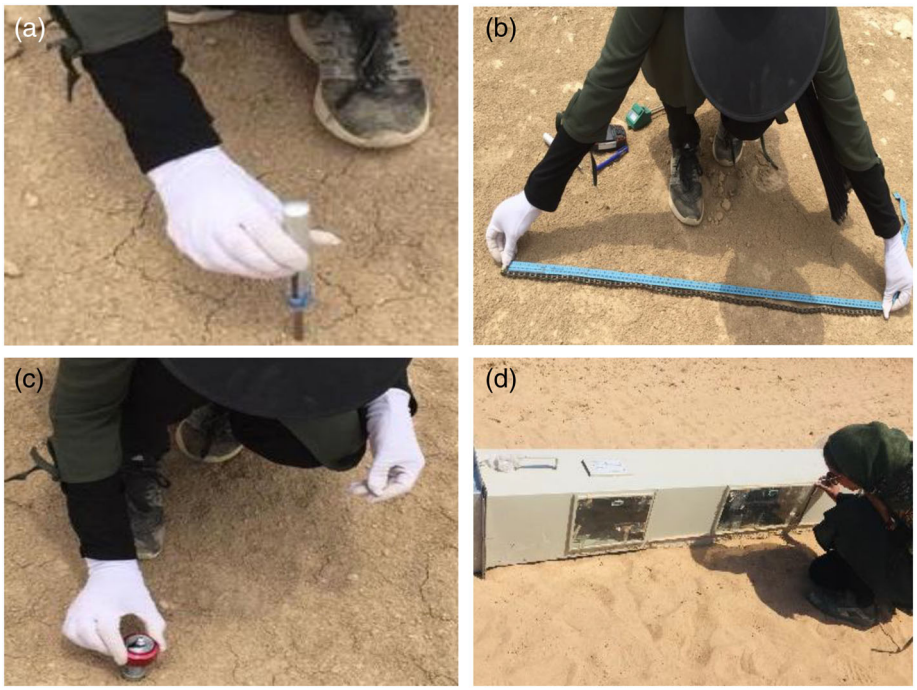

FIGURE 3 Measurement of soil mechanical properties at the 72 experimental sites in Fars Province, Iran in summer 2019. (a) Penetration resistance (PR), (b) soil surface roughness (SR), (c) shear strength (SS), and (d) view of the wind tunnel for measuring the threshold velocity (TV)

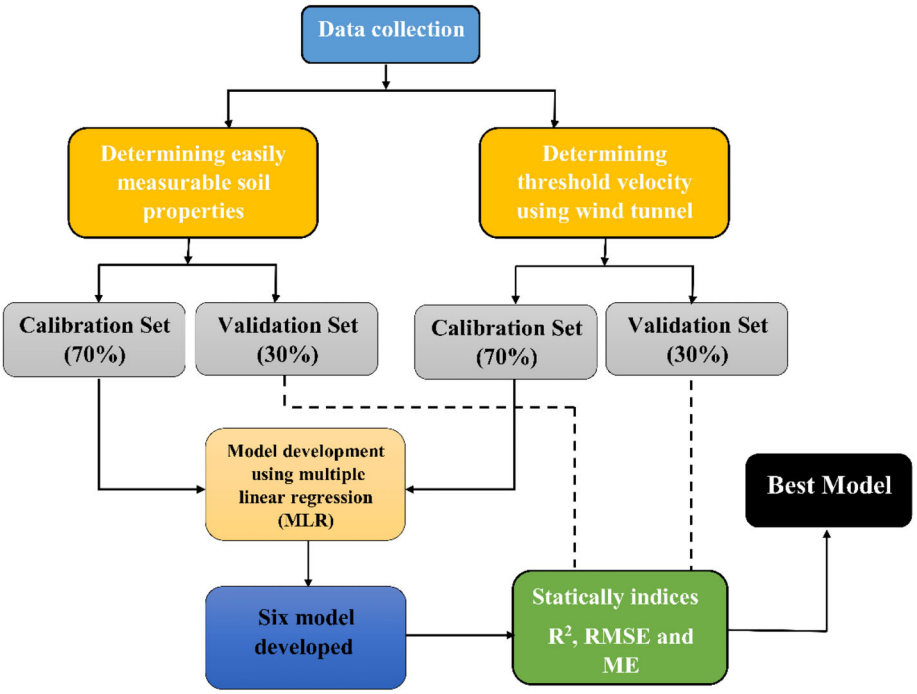

FIGURE 4 The flowchart of model development for predicting the threshold velocity (TV)

2.5 | Developing and validating PTFs

2.5.1 | Multiple linear regression

The flowchart of the modeling of TV by PTFs is given in Figure 4. Prior to the modelling, the data set was randomly divided into two groups: 70% ($\sim n = 50$) for models development and 30% ($\sim n = 22$) for models validation.

The MLR was used to model the TV using easily measurable lab- and field-based soil properties as follows:

$$y_i = B_0 + B_1 Xi_1 + B_2 Xi_2 + \ldots + B_n Xi_n + \in \quad (2)$$

Where:n is the number of observations, y_i is the *i*th TV, x_i is the *i*th explanatory variable, B_0 is the intercept (constant term), B_n is the slope coefficient for each explanatory variable, and ϵ is the model error term. The variance inflation index (VIF) was used to identify the collinearity between the input variables. A VIF value greater than 5 indicates a collinearity among variables and the weakness of the regression estimation. Besides, the *F*-test was used to test the significance of the regression model at the probability level of 5%.

TABLE 1 Descriptive statistics of the measured soil properties and wind erosion threshold velocity (TV), range (minimum–maximum), mean values, standard deviation (SD), and coefficient of variation (CV), for 72 sample sites in Fars Province, Iran

		Calibration data set ($n = 50$)			Validation data set ($n = 22$)		
Parameters	**Unit**	**Range**	**Mean ± SD**	**CV (%)**	**Range**	**Mean ± SD**	**CV (%)**
Clay	%	6.60–38.96	22.18[a] ± 6.06	27.32	6.60–36.96	23.50[a] ± 7.63	32.46
Silt	%	4.64–58.00	37.18[a] ± 12	32.27	6.00–52.36	33.57[a] ± 13.80	41.09
Sand	%	14.68–85.40	40.64[a] ± 15.85	39.01	10.68–87.40	42.93[a] ± 18.16	42.31
Aggregate mean weight diameter	mm	0.17–0.91	0.63[a] ± 0.13	20.38	0.30–0.90	0.67[a] ± 0.16	24.53
Soil organic matter	%	0.04–3.11	0.95[a] ± 0.62	65.64	0.13–3.20	1.14[a] ± 0.75	65.74
Calcium carbonate equivalent	%	38.93–92.31	55.13[a] ± 10.74	19.48	35.94–74.74	53.68[a] ± 9.70	18.06
Electrical conductivity	ds m^{-1}	0.0–189.71	16.76[a] ± 41.39	246.90	0.0–187.92	15.09[a] ± 40.62	269.21
Penetration resistance	kg cm^{-2}	0.50–2.70	1.56[a] ± 0.61	39.25	0.27–3.40	1.8[a] ± 0.78	43.25
Soil roughness	cm	0.21–0.85	0.52[a] ± 0.13	24.66	0.38–0.89	0.58[a] ± 0.15	26.34
Shear strength	kg cm^{-2}	0.03–2.50	1.40[a] ± 0.56	40.32	0.07–2.70	1.56[a] ± 0.75	47.90
Threshold velocity	m s^{-1}	3.00–12.33	7.90[a] ± 1.86	23.56	3.50–12.83	8.45[a] ± 2.37	27.98

[a]Significant difference ($p < 0.05$)

Statistical analyses were run by STATISTICA8 software (StatSoft, 2011). Descriptive statistics, including range (minimum–maximum), mean, standard deviation (SD), and coefficient of variation (CV) of soil properties, were calculated using SPSS software (Table 1).

2.6 | Statistical analysis

The relationships between easily measurable soil properties and TV were examined by the Pearson correlation test. The performance of the models was evaluated by the coefficient of determination (R^2), mean error (ME), and root mean square error (RMSE).

$$R^2 = \frac{\left[\sum_{i=1}^{n}\left(O_i - \overline{O_i}\right)\left(P_i - \overline{P_i}\right)\right]^2}{\sum_{i=1}^{n}\left(O_i - \overline{O_i}\right)^2 \sum_{i=1}^{n}\left(P_i - \overline{P_i}\right)^2} \quad (3)$$

$$ME = \sum\left(\frac{(P_i - O_i)}{n}\right) \quad (4)$$

$$RMSE = \sqrt{\left(\frac{\sum_{i=1}^{n}(P_i - O_i)^2}{n}\right)} \quad (5)$$

In these equations, P_i and O_i are the estimated and measured values of the parameter, respectively.

3 | RESULTS AND DISCUSSION

3.1 | Descriptive statistics of soil properties

The *t*-test showed that there was no significant difference between calibration and validation data sets ($p < 0.05$). According to Xu et al. (2014), CV < 10% and CV > 90% indicate low and high variability of a variable, respectively. All soil properties except EC had moderate variability (Table 1). Soil samples had great varieties in terms of texture including seven texture classes, indicating the abundance of medium textural classes (Figure 5). The MWD, which is reported as one of the most effective features in soil erosion (Kouchami-Sardoo et al., 2019), was 0.63 ± 0.13 and 0.67 ± 0.16 mm in the calibration and validation data sets, respectively. OM ranged from 0.04% to 3.20% with a mean value of 0.95% and 1.14% in the calibration and validation data sets, respectively, which are in agreement with the previous studies in the Fars Province (Ostovari et al., 2018; Sirjani et al., 2019). The mean CCE content was 55.13% and 53.68% in the calibration and validation

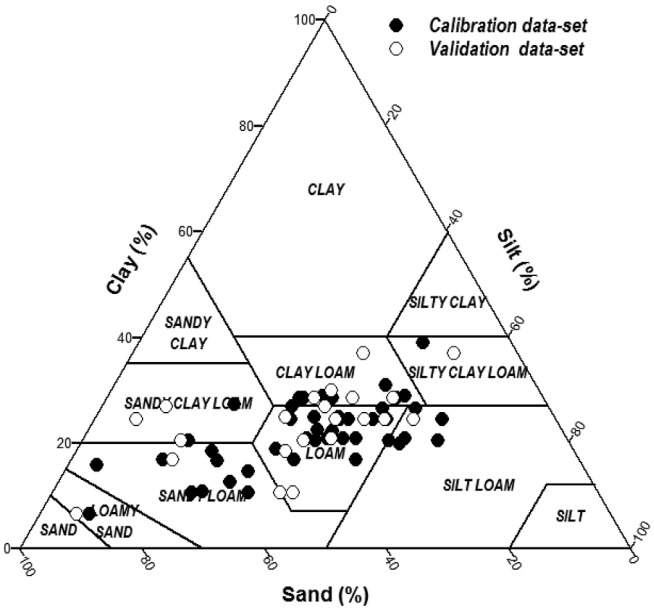

FIGURE 5 The USDA textural classes of the soils at the experimental sites in Fars Province, Iran

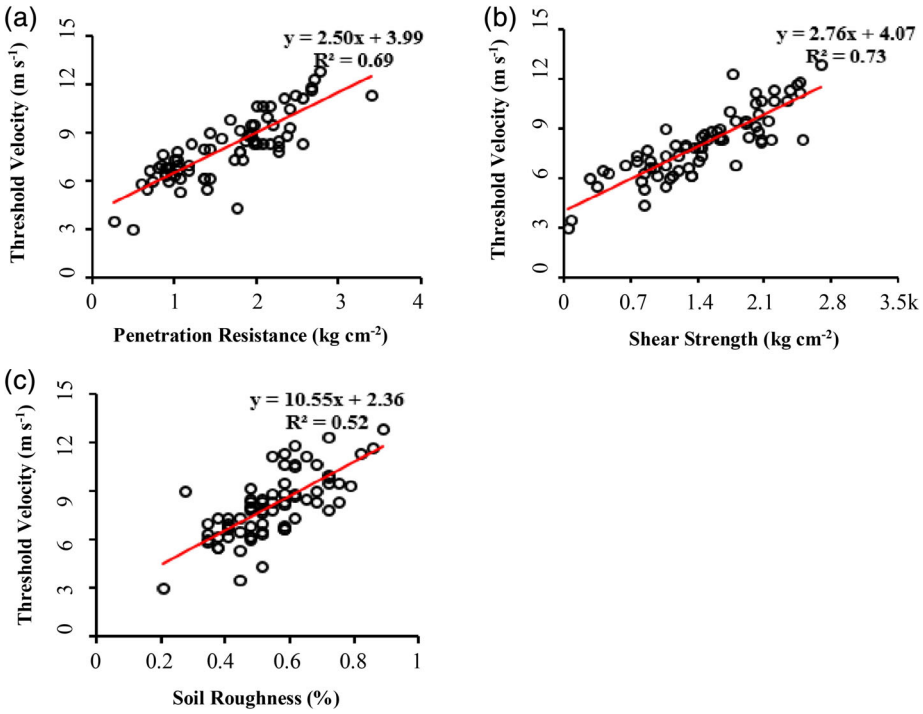

FIGURE 6 Threshold velocity (TV) and its relationship with soil mechanical properties ($N = 72$) in Fars Province, Iran

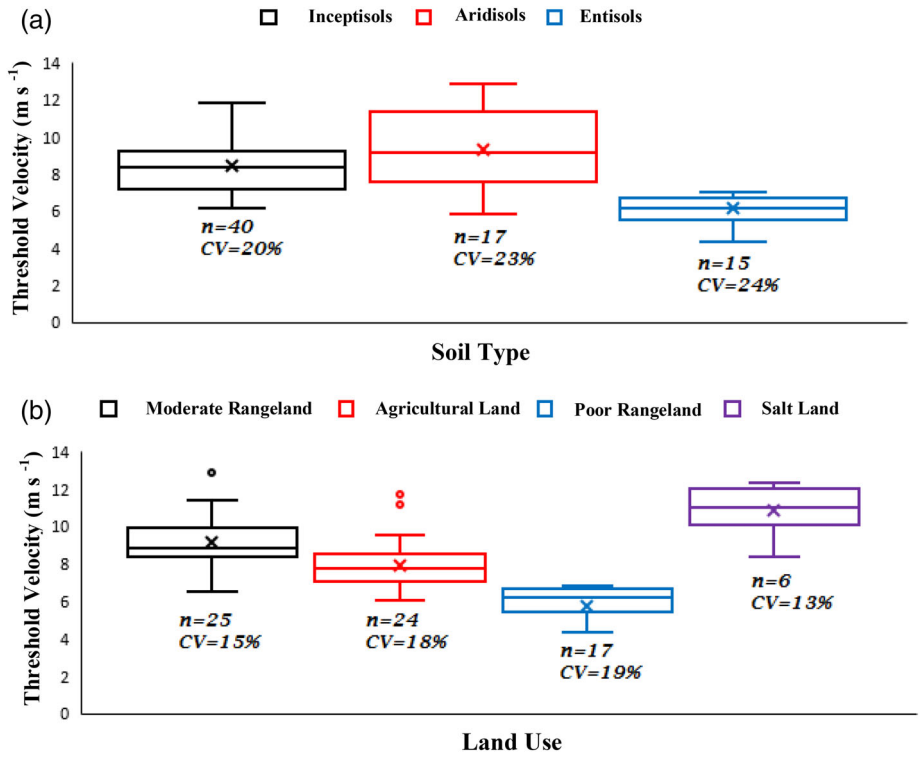

FIGURE 7 Box plot of threshold velocity (TV) in different (a) soil types and (b) land uses in Fars Province, Iran. CV, coefficient of variation; *N*, number of samples

data sets, respectively, which is consistent with previous reports in the calcareous soil of Fars Province (Ostovari et al., 2018, 2020; Sirjani et al., 2019). TV varied in the range of 3–12.83 m s^{-1} (at 0.25 m) in the study area, confirming a very different wind erosion potential across the study area. Considering a logarithmic wind profile and the roughness length generally reported for the desert areas (10^{-5} to 5 10^{-3} m) (i.e., Gillette et al., 1982; Greeley et al., 1997; Laurent et al., 2005; Marticorena et al., 1997; Sirjani et al., 2019), a wind velocity of 3 m s^{-1} at 0.25 m corresponds to wind velocity between 4.09 and 5.83 m s^{-1} at 10 m height. Likewise, a wind velocity of 12.83 m s^{-1} at 0.25 m corresponds to 17.50–24.93 m s^{-1}. These wind velocities can be found in Fars Province according to Figure 2, proving that wind erosion is a common process in this area.

TABLE 2 Pearson correlation matrix between soil properties in the study sites (Fars Province, Iran)

	Clay	Silt	Sand	MWD	OM	CCE	EC	PR	SR	SS
Silt	0.43**									
Sand	−0.72**	−0.93**								
MWD	0.81**	0.41**	−0.64**							
OM	0.40**	0.17	−0.29*	0.24*						
CCE	−0.54**	−0.26*	0.41**	−0.51**	−0.05					
EC	0.17	−0.02	−0.05	0.00	0.53**	0.25*				
PR	0.59**	0.24*	−0.41**	0.67**	0.23*	−0.39**	0.12			
SR	0.54**	0.17	−0.35**	0.59**	0.28*	−0.43**	0.13	0.68**		
SS	0.68**	0.26*	−0.47**	0.76**	0.26*	−0.43**	0.17	0.86**	0.75**	
TV	0.72**	0.26*	−0.48**	0.83**	0.30*	−0.45**	0.17	0.83**	0.72**	0.85**

Abbreviations: CCE, calcium carbonate equivalent; EC, electrical conductivity; MWD, aggregate mean weight diameter (dry aggregate stability); OM, organic matter; PR, penetration resistance; SR, soil roughness; SS, shear strength; TV, threshold velocity.
*$p < 0.05$; **$p < 0.01$

Figure 6 shows the relationship between soil mechanical properties (SR, SS, and PR) measured in the field and TV. As the values of soil mechanical properties increased, the TV values increased. Among the soil mechanical properties, SS had a stronger linear relationship with the TV ($R^2 = 0.73$), which shows the importance of SS against wind erosion.

Figure 7 shows the TV values in different soil types and land uses. The mean TV in Entisols ($n = 15$) was significantly ($p < 0.05$) lower than that in Aridisols and Inceptisols (Figure 7a). However, no significant difference was observed between Aridisols ($n = 17$) and Inceptisols ($n = 40$), indicating that Entisols have lower resistance to erosion compared to the other two soil types, which is similar to the results of Amini et al. (2009), Rashidi et al. (2011), and Ostovari et al. (2020). The fact that Entisols are more susceptible to wind erosion is due to the low soil-forming factors effects. They have not developed enough by weathering and they do not have any diagnostic horizons to make a good soil structure.

Land use had a significant effect ($p < 0.05$) on the TV (Figure 7b). Although the fundamental mechanism of wind erosion is the same for different land uses, soil surface properties vary greatly between them (Rezaei et al., 2016). According to Figure 7b, due to the low vegetation density and dry climate, the poor rangeland showed a lower TV (mean TV ~ 6 m s^{-1}) compared to other land uses. This is because soils of the poor rangeland had low MWD and OM, resulting in a lower resistance to wind erosion (Hajabbasi et al., 2008; Kouchami-Sardoo et al., 2020). While in moderate rangelands (mean TV ~ 9 m s^{-1}) and agricultural lands (mean TV ~ 8 m s^{-1}), soils had higher OM than poor rangelands (Figure 7b), due to the high amount of plant residual and root exudates. As a result, soil resistance to wind erosion and the TV were increased (Mirhasani et al., 2018). As shown in Figure 7b, the highest TV was found in the saline lands (mean TV ~ 11 m s^{-1}) where soils are more resistance to wind erosion, which can be explained by the high amount of bivalent cations such as calcium and magnesium that play the role as binding agents for flocculating the soil particles and creating large and stable aggregates (Kouchami-Sardoo et al., 2019). Moreover, the highest PR (1.74 kg cm^{-2}) was observed in saline lands which can be related to the formation of crust on the soil surface and was confirmed during field observations.

3.2 | Relationships between TV and soil properties

Table 2 shows the Pearson correlation matrix between soil physicochemical and mechanical properties and TV. The TV was positively and significantly correlated to SS ($r = 0.85$; $p < 0.01$; $n = 72$), PR ($r = 0.83$; $p < 0.01$; $n = 72$), MWD ($r = 0.83$; $p < 0.01$; $n = 72$), clay ($r = 0.72$; $p < 0.01$; $n = 72$), SR ($r = 0.72$, $p < 0.01$), OM ($r = 0.30$; $p < 0.05$; $n = 72$), and silt ($r = 0.26$; $p < 0.01$; $n = 72$). In addition, a negative and significant correlation was found between TV and sand ($r = -0.48$; $p < 0.01$; $n = 72$) and CCE ($r = -0.45$; $p < 0.01$; $n = 72$).

As shown in Table 2 and Figure 6, the SS, PR, and SR had a significant relationship with TV which is in consistent with the results of Mina et al. (2020) reporting an increase of TV with increasing the compressive and SS of soil. SR also reduces wind velocity by creating a barrier to wind flow, resulting in a decrease of wind erosion. In general, soil texture plays an important role in soil sensitivity to wind erosion (Pásztor et al., 2016). Sand particles ($r = -0.48$, $p < 0.05$) are easily separated and moved by wind force due to the lack of adhesion, but clay and silt particles are more resistant to wind erosion due to their adhesion (Li et al., 2015), this is also because sand is not able to form surface crust (Négyesi et al., 2021). As shown in Table 2, clay increases aggregation in the soil and thus reduces the movement of particles by the wind and increases the TV ($r = 0.72$). Moreover, TV showed a relatively high negative correlation with CCE ($r = -0.45$). This is also one of the factors that control the stability of soil structure, which can lead to the aggregation of primary particles. The effect of CCE on erosion depends on soil texture with CCE improving soil aggregation only in sandy and loamy sand soils. In contrast, no significant relationship was observed between soil erodibility factor and $CaCO_3$ content in Argentina (Colazo &

TABLE 3 The six developed pedotransfer functions (PTFs) for predicting threshold velocity (TV) (m s^{-1}) by the multiple linear regression for soils of Fars Province, Iran

				Calibration data set ($n = 50$)			Validation data set ($n = 22$)		
Model	Input variables	Developed model	VIF	R^2	RMSE (m s^{-1})	ME (m s^{-1})	R^2	RMSE (m s^{-1})	ME (m s^{-1})
PTF 1	Clay, Silt, Sand, and EC	TV = 2.73 + 0.23 (Clay)	1.00	0.57	1.20	−0.0008	0.42	1.79	−0.24
PTF 2	Clay, Silt, Sand, EC, and MWD	TV = 0.084 + 12.35 (MWD)	1.00	0.73	0.95	−0.0005	0.60	1.48	−0.15
PTF 3	Clay, Silt, Sand, EC, MWD, and OM	TV = 0.027 + 11.75 (MWD) + 0.45 (OM)	1.08	0.75	0.91	−0.0007	0.59	1.49	−0.10
PTF 4	Clay, Silt, Sand, EC, MWD, OM, and CCE	TV = 0.027 + 11.75 (MWD) + 0.45 (OM)	1.08	0.75	0.91	−0.0007	0.59	1.49	−0.10
PTF 5	PR, SR, and SS	TV = 3.85 + 1.63 (SS) + 1.14 (PR)	2.83	0.68	1.04	−0.0001	0.86	0.85	−0.007
PTF 6	All parameters	TV = 0.49 + 8.86 (MWD) + 1.15 (PR)	1.69	0.78	0.78	−0.0001	0.81	1.07	0.003

Abbreviations: CCE, calcium carbonate equivalent; EC, electrical conductivity; MWD, aggregate mean weight diameter (dry aggregate stability); OM, organic matter; PR, penetration resistance; SR, soil roughness; SS, shear strength; TV, threshold velocity.

Buschiazzo, 2010). In addition, soil OM increases soil aggregation stability, resulting in an increase in the TV ($r = 0.30$). The OM is one of the most important soil properties that acts as a binding agent for primary soil particles in aggregate formation (Duan et al., 2017; Négyesi et al., 2016; Sirjani et al., 2019).

3.3 | Development and validation of models to predict TV

The most important principle for developing PTFs is to provide a simple model with a low number of independent easily measurable soil properties. With emphasis on the use of a minimum number of easily measurable soil properties, six scenarios were considered for modeling TV. Finally, six PTFs were developed using the MLR method.

Table 3 presents the six developed PTFs and the performance criteria of the PTFs in both calibration and validation data sets. The input variables used for PTF 1 include soil texture (clay, silt, and sand) and EC (considering as the most common available soil properties); however, only clay appeared in PTF 1 (Table 3). This could be due to the existence of a strong significant correlation between TV and clay (Table 2). As shown in Table 3, for both calibration and validation data sets, PTF 1 with the lower R^2 and the highest RMSE provided the poorest results in predicting the TV. PTF 2 was developed by adding MWD to PTF 1. Interestingly, only MWD appeared in PTF 2. The impact of clay (Mahmoodabadi & Rajabpour, 2017; Pásztor et al., 2016; Van Pelt et al., 2017) and MWD (Kouchami-Sardoo et al., 2019; Zamani & Mahmoodabadi, 2013) on TV have been reported in many studies. PTF 3 was developed by adding OM to PTF 2. Against PTF 2, both MWD and OM appeared in PTF 3. Soil OM increases aggregation by playing a role as a binding agent between soil particles (Duan et al., 2017; Ostovari et al., 2020), as a result increasing the TV (Sirjani et al., 2019). Consequently, PTF 4 was developed by adding CCE to PTF 3. Similar to PTF3, two variables of MWD and OM appeared in PTF 4 with the same coefficients, indicating that CCE is not as important as MWD and OM for predicting the TV. This is because soils are mostly calcareous in the study area. PTF 5 was developed using only soil mechanical properties (SS, PR, and SR). It is worth mentioning that although SS, PR, and SR were significantly correlated with the TV, only SS and PR appeared in PTF 5. The significant influence of SS (Mina et al., 2020; Naghizade Asl et al., 2019), PR (Kouchami-Sardoo et al., 2020), and SR (Sirjani et al., 2019; Yan et al., 2015) on soil erosion have been pointed out in several studies. According to the criteria indices in the validation data set ($R^2 = 0.86$ and RMSE = 0.85 m s^{-1}), PTF 5 showed a good performance in predicting the TV. Finally, PTF 6 was developed using all parameters (clay, silt, sand, EC, MWD, OM, CCE, SR, PR, and SS). However, only two variables of MWD and PR appeared in the developed model (Table 3). As previously mentioned, MWD and PR are significantly linked to soil erosion.

Measured TV values and predicted by different PTFs in both calibration and validation sets are shown in Figure 8. As shown in Figures 8e,f, among PFTs, points of both PTF 5 and PTF 6 were well around the 1: 1 line.

In general, PTF 5 ($R^2 = 0.86$, RMSE = 0.85 m s^{-1}, and ME = −0.007 m s^{-1}) and PTF 6 ($R^2 = 0.81$, RMSE = 1.07 m s^{-1}, and ME = 0.003 m s^{-1}) with excellent performance criteria were the best models for the TV prediction (Table 3). However, we preferred selecting PTF 5, which was developed based on only the soil mechanical properties (PR and SS), as the best model for predicting the TV. This is because measuring mechanical properties only requires simple field measurements without additional sampling or chemical laboratory measurements. This is especially important for predicting the spatial distribution of TV on a large scale. Furthermore, determination of these soil mechanical properties is conducted using portable, inexpensive, prompt, easy to use and environmental friendly devices. Other studies have

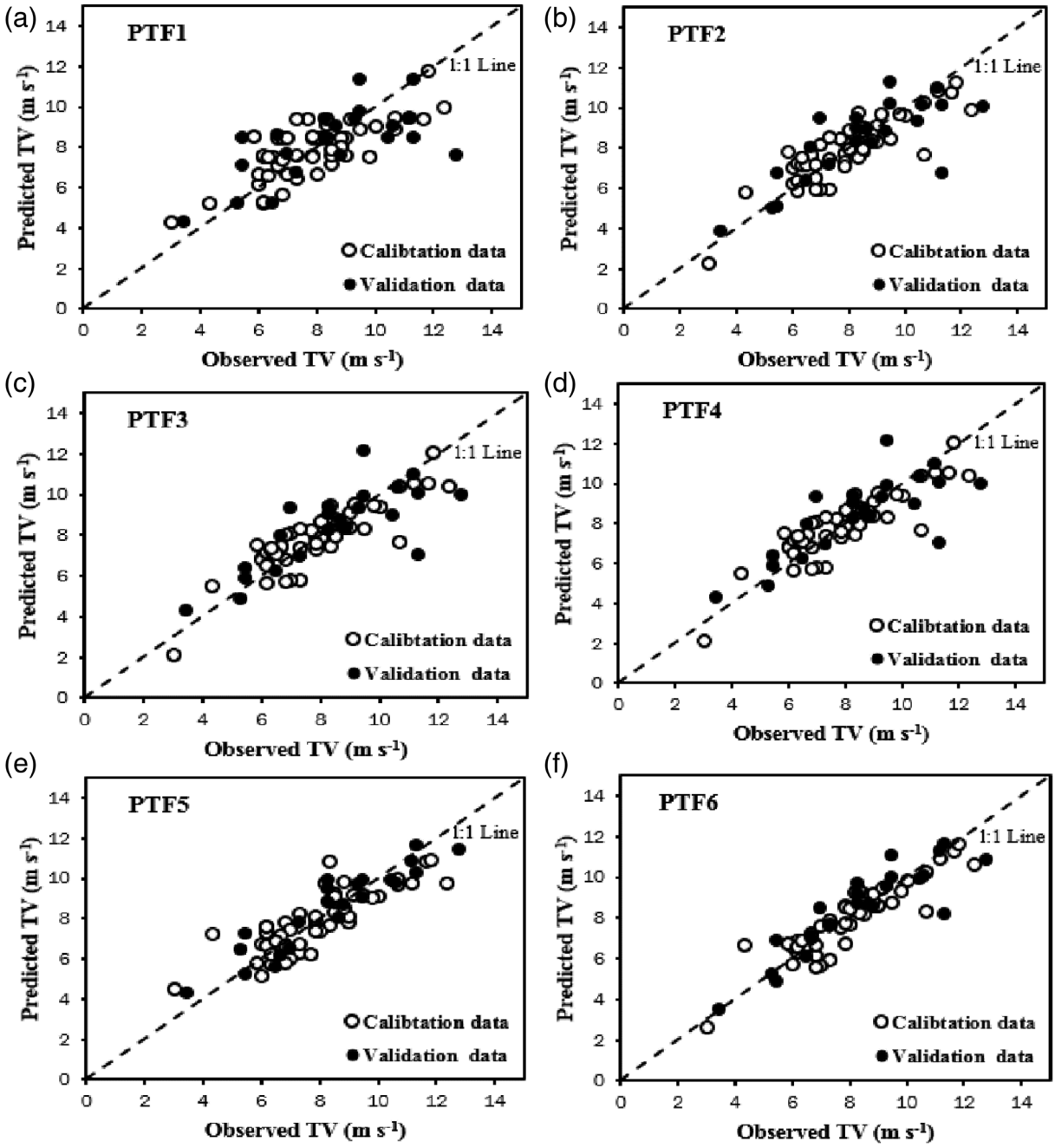

FIGURE 8 Scatter plots of predicted and measured threshold velocity (TV) by all proposed pedotransfer functions (PTFs). (a) Calibration data set ($N = 50$) and (b) validation data set ($N = 22$)

shown that the MLR is a reliable method in predicting some soil properties, for example for predicting soil erodibility (Ostovari et al., 2018; Raei et al., 2020), TV (Li et al., 2010), soil cation exchange capacity (Ghorbani et al., 2015), and soil loss tolerance (Ostovari et al., 2018).

4 | CONCLUSION

TV is a very important parameter for indicating soil wind erosion potential in arid and semiarid regions. Therefore, this study was conducted to determine the TV using a portable wind tunnel and to develop some PTFs to predict the TV using easily measurable soil properties. Six PTFs were developed based on the easily measurable soil properties as the input variables. Results showed that the TV varied from 3.0 m s^{-1} (in poor rangelands and Entisols) to 12.83 m s^{-1} (in saline lands and Aridisols). Results also revealed that the MWD and PR as input variables significantly increased the performance of the PTFs due to the high correlation between MWD and PR and the TV ($r = 0.83$ and $r = 0.83$, respectively). According to statistical indices ($R^2 = 0.86$ and 0.81; RMSE = 0.85 and 1.07 m s^{-1} for the validation

data set of PTF 5 and PTF 6, respectively), PTF5 and PTF6 yielded the best performances for TV prediction. However, because of practical considerations, PTF5 is preferred over PTF6 since it only needs simple and easily measurable mechanical soil properties which is important for predicting TV in large areas prone to wind erosion. The results from this study can be useful for efficiently assessing vast areas prone to wind erosion and dust emission and can help the policymakers to prioritize areas for soil conservation practices. The latter is very important for developing countries where only limited budget is available for soil conservation programs. In addition, portable wind tunnel is not always available for wind erosion studies, such fast and easy-to-apply methods introduced in this study can be a good alternative for wind erosion monitoring without disturbing the soil.

DATA AVAILABILITY STATEMENT

The data that support the findings of this study are available from the corresponding author, upon reasonable request.

ORCID

Mahrooz Rezaei https://orcid.org/0000-0002-9413-6034

REFERENCES

Abbasi, S., Rezaei, M., Keshavarzi, B., Mina, M., Ritsema, C., & Geissen, V. (2021). Investigation of the 2018 Kouchami-Sardoo et alShiraz dust event: Potential sources of metals, rare earth elements, and radionuclides; health assessment. *Chemosphere*, *279*, 130533. https://doi.org/10.1016/j.chemosphere.2021.130533

Amini, J. H., Naseri, M. Y., Khormali, F., & Movahedi, N. S. (2009). Variations in properties of the loess derived soils as affected by geomorphic positions in two different climatic regions of Golestan Province. *Journal of Water and Soil Conservation (Journal of Agricultural Sciences and Natural Resources)*., *16*(1), 1–17 (In Persian).

Azimzadeh, H. R., Ekhtesasi, M. R., Refahi, H. G., Rohipour, H., & Gorji, M. (2008). Wind erosion measurement on fallow lands of Yazd-Ardakan Plain, Iran. *Desert*, *13*(2), 167–174.

Belnap, J., Phillips, S. L., Herrick, J. E., & Johansen, J. R. (2007). Wind erodibility of soils at Fort Irwin, California (Mojave Desert), USA, before and after trampling disturbance: Implications for land management. *Earth Surface Processes and Landforms: The Journal of the British Geomorphological Research Group*., *32*(1), 75–84. https://doi.org/10.1002/esp.1372

Bento, C. P., Goossens, D., Rezaei, M., Riksen, M., Mol, H. G., Ritsema, C. J., & Geissen, V. (2017). Glyphosate and AMPA distribution in wind-eroded sediment derived from loess soil. *Environmental Pollution*., *220*, 1079–1089. https://doi.org/10.1016/j.envpol.2016.11.033

Bradford, J. M. (1986). Penetrability. *Methods of Soil Analysis: Part 1 Physical and Mineralogical Methods*, *5*, 463–478.

Brahim, N., Bernoux, M., & Gallali, T. (2012). Pedotransfer functions to estimate soil bulk density for Northern Africa: Tunisia case. *Journal of Arid Environments*, *81*, 77–83. https://doi.org/10.1016/j.jaridenv.2012.01.012

Chappell, A., Webb, N. P., Guerschman, J. P., Thomas, D. T., Mata, G., Handcock, R. N., & Butler, H. J. (2018). Improving ground cover monitoring for wind erosion assessment using MODIS BRDF parameters. *Remote Sensing of Environment*., *204*, 756–768. https://doi.org/10.1016/j.rse.2017.09.026

Chepil, W. S. (1950). Properties of soil which influence wind erosion. II. Dry aggregate structure as an index of erodibility. *Soil Science*, *69*, 403–414. https://doi.org/10.1016/j.rse.2017.09.026

Colazo, J. C., & Buschiazzo, D. E. (2010). Soil dry aggregate stability and wind erodible fraction in a semiarid environment of Argentina. *Geoderma*, *159*(1–2), 228–236. https://doi.org/10.1016/j.geoderma.2010.07.016

Duan, X., Shi, X., Li, Y., Rong, L., & Fen, D. (2017). A new method to calculate soil loss tolerance for sustainable soil productivity in farmland. *Agronomy for Sustainable Development*, *37*(2), 2–13. https://doi.org/10.1007/s13593-016-0409-3

Ghorbani, H., Kashi, H., & Moghadas, N. (2015). Estimation of soil cation exchange capacity using multiple regression, artificial neural networks, and adaptive neuro-fuzzy inference system models in Golestan Province, Iran. *Communications in Soil Science and Plant Analysis*., *46*(6), 763–780. https://doi.org/10.1080/00103624.2015.1006367

Gillette, D. A., Adams, J., Muhs, D., & Kihl, R. (1982). Threshold friction velocities and rupture moduli for crusted desert soils for the input of soil particles into the air. *Journal of Geophysical Research: Oceans*, *87*(C11), 9003–9015. https://doi.org/10.1029/JC087iC11p09003

Gillies, J. A., Nickling, W. G., & King, J. (2006). Aeolian sediment transport through large patches of roughness in the atmospheric inertial sublayer. *Journal of Geophysical Research: Earth Surface*, *111*(F2), 1–13. https://doi.org/10.1029/2005JF000434

Greeley, R., Blumberg, D. G., McHone, J. F., Dobrovolskis, A., Iversen, J. D., Lancaster, N., Rasmussen, K. R., Wall, S. D., & White, B. R. (1997). Applications of spaceborne radar laboratory data to the study of aeolian processes. *Journal of Geophysical Research: Planets*, *102*(E5), 10971–10983. https://doi.org/10.1029/97JE00518

Hajabbasi, M. A., Besalatpour, A., & Melali, A. R. (2008). Impacts of converting rangelands to cultivated land on physical and chemical properties of soils in west and southwest of Isfahan. *Journal of Water and Soil Science*., *11*(42), 525–534 (In Persian).

Hoogsteen, M. J., Lantinga, E. A., Bakker, E. J., Groot, J. C., & Tittonell, P. A. (2015). Estimating soil organic carbon through loss on ignition: Effects of ignition conditions and structural water loss. *European Journal of Soil Science*., *66*(2), 320–328. https://doi.org/10.1111/ejss.12224

Kashi, H., Emamgholizadeh, S., & Ghorbani, H. (2014). Estimation of soil infiltration and cation exchange capacity based on multiple regression, ANN (RBF, MLP), and ANFIS models. *Communications in Soil Science and Plant Analysis*, *45*(9), 1195–1213. https://doi.org/10.1080/00103624.2013.874029

Kemper, W. D., & Rosenau, R. C. (1986). Aggregate stability and size distribution. *Methods of Soil Analysis: Part 1 Physical and Mineralogical Methods*, *5*, 425–442.

Kheirabadi, H., Mahmoodabadi, M., Jalali, V., & Naghavi, H. (2018). Sediment flux, wind erosion and net erosion influenced by soil bed length, wind velocity and aggregate size distribution. *Geoderma*, *323*, 22–30. https://doi.org/10.1016/j.geoderma.2018.02.042

Kouchami-Sardoo, I., Shirani, H., Esfandiarpour-Boroujeni, I., Álvaro-Fuentes, J., & Shekofteh, H. (2019). Optimal feature selection for prediction of wind erosion threshold friction velocity using a modified evolution algorithm. *Geoderma*, *354*, 1–12. https://doi.org/10.1016/j.geoderma.2019.07.031

Kouchami-Sardoo, I., Shirani, H., Esfandiarpour-Boroujeni, I., Besalatpour, A. A., & Hajabbasi, M. A. (2020). Prediction of soil wind erodibility using a hybrid genetic algorithm—Artificial neural network method. *Catena*, *187*, 104315. https://doi.org/10.1016/j.catena.2019.104315

Kumar, M., Bandyopadhyay, A., Raghuwanshi, N. S., & Singh, R. (2008). Comparative study of conventional and artificial neural network-based ETo estimation models. *Irrigation Science*, *26*(6), 531–545. https://doi.org/10.1007/s00271-008-0114-3

Laurent, B., Marticorena, B., Bergametti, G., Chazette, P., Maignan, F., & Schmechtig, C. (2005). Simulation of the mineral dust emission frequencies from desert areas of China and Mongolia using an aerodynamic roughness length map derived from the POLDER/ADEOS

1 surface products. *Journal of Geophysical Research: Atmospheres*, *110*(D18), 1–21. https://doi.org/10.1029/2004JD005013

Li, J., Flagg, C., Okin, G. S., Painter, T. H., Dintwe, K., & Belnap, J. (2015). On the prediction of threshold friction velocity of wind erosion using soil reflectance spectroscopy. *Aeolian Research*, *19*, 129–136. https://doi.org/10.1016/j.aeolia.2015.10.001

Li, J., Okin, G. S., Herrick, J. E., Belnap, J., Munson, S. M., & Miller, M. E. (2010). A simple method to estimate threshold friction velocity of wind erosion in the field. *Geophysical Research Letters*, *37*(10), 1-5. https://doi.org/10.1029/2010GL043245

Liao, K. H., Xu, S. H., Wu, J. C., Ji, S. H., & Lin, Q. (2011). Assessing soil water retention characteristics and their spatial variability using pedotransfer functions. *Pedosphere*, *21*, 413–422. https://doi.org/10.1016/S1002-0160(11)60143-4

Mahmoodabadi, M., & Rajabpour, H. (2017). Study on the effect of initial soil moisture content on wind erosion rate using a laboratory wind tunnel. *Journal of Water and Soil Conservation*, *24*(2), 167–183 (In Persian).

Marticorena, B., Bergametti, G., Gillette, D., & Belnap, J. (1997). Factors controlling threshold friction velocity in semiarid and arid areas of the United States. *Journal of Geophysical Research: Atmosphres*, *102*(D19), 23277–23287. https://doi.org/10.1029/97JD01303

Mazidi, A., Jafari Zoj, F., & Heidary, S. (2015). Simulation of dust storm events on February 28, 2009 in Fars Province usingthe WRF model. *Theoretical and Applied Climatology*, *2*(2), 49–68.

Mina, M., Emami, H., & Karimi, A. (2020). Evaluation the efficiency of different mulches to combat wind erosion of sandy soil running title: Efficiency of different mulches to control wind erosion. *Sustainable Earth Review*, *1*(1), 16–22. https://doi.org/10.52547/sustainearth.1.1.16

Mina, M., Rezaei, M., Sameni, A., Moosavi, A. A., & Ritsema, C. (2021). Vis-NIR spectroscopy predicts threshold velocity of wind erosion in calcareous soils. *Geoderma*, *401*, 1–11. https://doi.org/10.1016/j.geoderma.2021.115163

Mirhasani, M., Rostami, N., Bazgir, M., & Tavakoli, M. (2018). An investigation of land-use effect on dust concentration and soil loss in desert areas: A case of Ein Khosh-Dehloran, Ilam. *Environmental Erosion Research Journal*, *8*(1), 1–20.

Moazenzadeh, R., & Ghahraman, B. (2016). Prediction of some soil hydraulic properties using Pedotransfer function. *Environmental Erosion Research Journal*, *24*, 47–63.

Moradi, H. R., Rajabi, M., & Faragzadeh, M. (2011). Investigation of meteorological drought characteristics in Fars Province, Iran. *Catena*, *84*(1–2), 35–46. https://doi.org/10.1016/j.catena.2010.08.016

Moreno, R. G., Álvarez, M. C., Tarquis, A. M., González, A. P., & Requejo, A. S. (2010). Shadow analysis of soil surface roughness compared to the chain set method and direct measurement of micro-relief. *Biogeosciences*, *7*(1), 2477–2487. https://doi.org/10.5194/bg-7-2477-2010

Morshedi Nodej, T., & Rezazadeh, M. (2018). The spatial distribution of critical wind erosion centers according to the dust event in Hormozgan province (south of Iran). *Catena*, *167*, 340–352. https://doi.org/10.1016/j.catena.2018.05.008

Munkhtsetseg, E., Shinoda, M., Gillies, J. A., Kimura, R., King, J., & Nikolich, G. (2016). Relationships between soil moisture and dust emissions in a bare sandy soil of Mongolia. *Particuology*, *28*, 131–137. https://doi.org/10.1016/j.partic.2016.03.001

Naghizade Asl, F. N., Asgari, H. R., Emami, H., & Jafari, M. (2019). Combined effect of micro silica with clay, and gypsum as mulches on shear strength and wind erosion rate of sands. *International Soil and Water Conservation Research*, *7*(4), 388–394. https://doi.org/10.1016/j.iswcr.2019.03.003

Natural Resources and Forestry Organization of Fars Province. (2019). Detailed Report of Fars Province. Fars Department of Desert Management, Shiraz, Iran (in Persian).

Négyesi, G., Lóki, J., Buró, B., & Szabó, S. (2016). Effect of soil parameters on the threshold wind velocity and maximum eroded mass in a dry environment. *Arabian Journal of Geosciences*, *9*(11), 588. https://doi.org/10.1007/s12517-016-2626-0

Négyesi, G., Szabó, S., Buró, B., Mohammed, S., Lóki, J., Rajkai, K., & Holb, I. J. (2021). Influence of soil moisture and crust formation on soil evaporation rate: A wind tunnel experiment in Hungary. *Agronomy*, *11*(5), 935. https://doi.org/10.3390/agronomy11050935

Nelson, R. E. (1982). Carbonate and gypsum. In A. L. Page (Ed.), *Methods of soil analysis: Part 1. Agronomy handbook 9* (Vol. 6, pp. 181–197). Madison, WI: American Society of Agronomy and Soil Science Society of America.

Ostovari, Y., Ghorbani-Dashtaki, S., Bahrami, H. A., Abbasi, M., Dematte, J. A. M., Arthur, E., & Panagos, P. (2018). Towards prediction of soil erodibility, SOM and CaCO3 using laboratory Vis-NIR spectra: A case study in a semi-arid region of Iran. *Geoderma*, *314*, 102–112. https://doi.org/10.1016/j.geoderma.2017.11.014

Ostovari, Y., Ghorbani-Dashtaki, S., Bahrami, H. A., Naderi, M., Dematte, J. A. M., & Kerry, R. (2016). Modification of the USLE K factor for soil erodibility assessment on calcareous soils in Iran. *Geomorphology*, *273*, 385–395. https://doi.org/10.1016/j.geomorph.2016.08.003

Ostovari, Y., Moosavi, A. A., & Pourghasemi, H. R. (2020). Soil loss tolerance in calcareous soils of a semiarid region: Evaluation, prediction, and influential parameters. *Land Degradation & Development*, *31*, 1–12. https://doi.org/10.1002/ldr.3597

Page, A. L., Miller, R. H., & Jeeney, D. R. (1992). Methods of soil analysis, part 1. In *Physical and mineralogical methods* (1750). Madison, WI: Soil Science Society of American Publication.

Pásztor, L., Négyesi, G., Laborczi, A., Kovács, T., László, E., & Bihari, Z. (2016). Integrated spatial assessment of wind erosion risk in Hungary. *Natural Hazards and Earth System Sciences*, *16*(16), 2421–2432. https://doi.org/10.5194/nhess-16-2421-2016

Raei, B., Ahmadi, A., Neyshaburi, M. R., Ghorbani, M. A., & Asadzadeh, F. (2020). Evaluating efficiency of some artificial intelligence techniques for modeling soil wind Erodibility in part of eastern land of Urmia Lake. *Iranian Journal of Soil and Water Research*, *51*(1), 61–76.

Rashidi, Z., Esfandiarpoor Borujeni, I., Abasspoor, A. and Kamali, A. (2011). The effects of erosion on the soil classification of different hill-land positions, East of Damavand, Tehran. Paper presented at the 11th Conference on Erosion and Sediment, Kerman, Iran.

Rezaei, M., Riksen, M. J. P. M., Sirjani, E., Sameni, A., & Geissen, V. (2019). Wind erosion as a driver for transport of light density microplastics. *Science of the Total Environment*, *669*, 273–281. https://doi.org/10.1016/j.scitotenv.2019.02.382

Rezaei, M., Sameni, A., Fallah Shamsi, S. R., & Bartholomeus, H. (2016). Remote sensing of land use/cover changes and its effect on wind erosion potential in southern Iran. *PeerJ*, *4*, e1948. https://doi.org/10.7717/peerj.1948

Saleh, A. (1993). Soil roughness measurement: Chain method. *Journal of Soil and Water Conservation*, *48*(6), 527–529.

Sankey, J. B., Glenn, N. F., Germino, M. J., Gironella, A. I. N., & Thackray, G. D. (2010). Relationships of aeolian erosion and deposition with LiDAR-derived landscape surface roughness following wildfire. *Geomorphology*, *119*(1–2), 135–145. https://doi.org/10.1016/j.geomorph.2010.03.013

Shao, Y. (2008). *Physics and modelling of wind erosion* (Vol. 37). Cham, CH: Springer Science & Business Media.

Sharratt, B. S., & Vaddella, V. (2014). Threshold friction velocity of crusted windblown soils in the Columbia Plateau. *Aeolian Research*, *15*, 227–234. https://doi.org/10.1016/j.aeolia.2014.08.002

Shi, P., Castaldi, F., van Wesemael, B., & Van Oost, K. (2020). Vis-NIR spectroscopic assessment of soil aggregate stability and aggregate size distribution in the Belgian Loam Belt. *Geoderma*, *357*, 1–9. https://doi.org/10.1016/j.geoderma.2019.113958

Sirjani, E., Sameni, A., Moosavi, A. A., Mahmoodabadi, M., & Laurent, B. (2019). Portable wind tunnel experiments to study soil erosion by wind

and its link to soil properties in Fars Province, Iran. *Geoderma*, *333*, 69–80. https://doi.org/10.1016/j.geoderma.2018.07.012

StatSoft, I., 2011. STATISTICA (data analysis software system).

Sweeney, M. R., Zlotnik, V. A., Joeckel, R. M., & Stout, J. E. (2016). Geomorphic and hydrologic controls of dust emissions during drought from Yellow Lake Playa, West Texas, USA. *Journal of Arid Environments*, *133*, 37–46. https://doi.org/10.1016/j.jaridenv.2016.05.007

Van Pelt, R. S., Hushmurodov, S. X., Baumhardt, R. L., Chappell, A., Nearing, M. A., Polyakov, V. O., & Strack, J. E. (2017). The reduction of partitioned wind and water erosion by conservation agriculture. *Catena*, *148*, 160–167. https://doi.org/10.1016/j.catena.2016.07.004

Van Pelt, R. S., & Zobeck, T. M. (2013). Portable wind tunnels for fields testing of soils and natural surfaces. In *Wind tunnels designs and their diverse engineering applications* (pp. 59–73). London: InTech.

Vázquez, E. V., Miranda, J. V., & González, A. P. (2005). Characterizing anisotropy and heterogeneity of soil surface microtopography using fractal models. *Ecological Modelling*, *182*(3–4), 337–353. https://doi.org/10.1016/j.ecolmodel.2004.04.012

Von Holdt, J. R. C., Eckardt, F. D., Baddock, M. C., & Wiggs, G. F. (2019). Assessing landscape dust emission potential using combined ground-based measurements and remote sensing data. *Journal of Geophysical Research: Earth Surface*, *124*(5), 1080–1098. https://doi.org/10.1029/2018JF004713

Wagner, B., Tarnawski, V. R., Hennings, V., Muller, U., Wessolek, G., & Plagge, R. (2001). Evaluation of pedotransfer function for unsaturated soil hydraulic conductivity using an independent data set. *Geoderma*, *102*, 275–297.

Xu, G., Li, Z., Li, P., Zhang, T., & Cheng, S. (2014). Spatial variability of soil available phosphorus in a typical watershed in the source area of the middle Dan River, China. *Environmental Earth Sciences*, *71*(9), 3953–3962.

Yan, Y., Wu, L., Xin, X., Wang, X., & Yang, G. (2015). How rain-formed soil crust affects wind erosion in a semi-arid steppe in northern China. *Geoderma*, *249*, 79–86. https://doi.org/10.1016/j.geoderma.2015.03.011

Zamani, S., & Mahmoodabadi, M. (2013). Effect of particle-size distribution on wind erosion rate and soil erodibility. *Archives of Agronomy and Soil Science*, *59*(12), 1743–1753. https://doi.org/10.1080/03650340.2012.748984

Zhang, C., Wang, X., Zou, X., Tian, J., Liu, B., Li, J., & Wu, Y. (2018). Estimation of surface shear strength of undisturbed soils in the eastern part of northern China's wind erosion area. *Soil and Tillage Research*, *178*, 1–10. https://doi.org/10.1016/j.still.2017.12.014

Zhang, Y. M., Wang, H. L., Wang, X. Q., Yang, W. K., & Zhang, D. Y. (2006). The microstructure of microbiotic crust and its influence on wind erosion for a sandy soil surface in the Gurbantunggut Desert of Northwestern China. *Geoderma*, *132*(3–4), 441–449. https://doi.org/10.1016/j.geoderma.2005.06.008

How to cite this article: Rezaei, M., Mina, M., Ostovari, Y., & Riksen, M. J. P. M. (2022). Determination of the threshold velocity of soil wind erosion using a wind tunnel and its prediction for calcareous soils of Iran. *Land Degradation & Development*, 1–13. https://doi.org/10.1002/ldr.4309